EXTENDED PDF FORMAT
SPONSORED BY
Announcing Enhanced Product Information Pages!
Evaluate our Data. Review Published Results.
Make a Confident Choice.
Learn more
R&D SYSTEMS
www.rndsystems.com/PSP

Soft Matter Models of Developing Tissues and Tumors

David Gonzalez-Rodriguez *et al.*

Science **338**, 910 (2012);
DOI: 10.1126/science.1226418

This copy is for your personal, non-commercial use only.

If you wish to distribute this article to others, you can order high-quality copies for your colleagues, clients, or customers by clicking here.

Permission to republish or repurpose articles or portions of articles can be obtained by following the guidelines here.

The following resources related to this article are available online at www.sciencemag.org (this information is current as of December 20, 2012):

Updated information and services, including high-resolution figures, can be found in the online version of this article at:
http://www.sciencemag.org/content/338/6109/910.full.html

A list of selected additional articles on the Science Web sites **related to this article** can be found at:
http://www.sciencemag.org/content/338/6109/910.full.html#related

This article **cites 76 articles**, 20 of which can be accessed free:
http://www.sciencemag.org/content/338/6109/910.full.html#ref-list-1

This article appears in the following **subject collections:**
Materials Science
http://www.sciencemag.org/cgi/collection/mat_sci

Downloaded from www.sciencemag.org on December 20, 2012

Science (print ISSN 0036-8075; online ISSN 1095-9203) is published weekly, except the last week in December, by the American Association for the Advancement of Science, 1200 New York Avenue NW, Washington, DC 20005. Copyright 2012 by the American Association for the Advancement of Science; all rights reserved. The title *Science* is a registered trademark of AAAS.

15. C. Lipinski, *Am. Pharm. Rev.* **5**, 82 (2002).
16. P. P. Adiseshaiah, J. B. Hall, S. E. McNeil, *Wiley Interdiscip. Rev. Nanomed. Nanobiotechnol.* **2**, 99 (2010).
17. E. A. Murphy *et al.*, *Proc. Natl. Acad. Sci. U.S.A.* **105**, 9343 (2008).
18. Y. J. Yu *et al.*, *Sci. Transl. Med.* **3**, 84ra44 (2011).
19. J. Yang *et al.*, *Angew. Chem. Int. Ed.* **46**, 8836 (2007).
20. Y. P. Luo *et al.*, *J. Clin. Invest.* **116**, 2132 (2006).
21. M. B. Yatvin, W. Kreutz, B. A. Horwitz, M. Shinitzky, *Science* **210**, 1253 (1980).
22. E. Lallana, A. Sousa-Herves, F. Fernandez-Trillo, R. Riguera, E. Fernandez-Megia, *Pharm. Res.* **29**, 1 (2012).
23. K. M. McNeeley, A. Annapragada, R. V. Bellamkonda, *Nanotechnology* **18**, 385101 (2007).
24. T. M. Allen, *Nat. Rev. Cancer* **2**, 750 (2002).
25. J. Y. Yang *et al.*, *Cell Biochem. Biophys.* **62**, 221 (2012).
26. R. W. Cho, M. F. Clarke, *Curr. Opin. Genet. Dev.* **18**, 48 (2008).
27. A. van Waarde *et al.*, *J. Nucl. Med.* **48**, 1320 (2007).
28. W. Jiang, B. Y. S. Kim, J. T. Rutka, W. C. W. Chan, *Nat. Nanotechnol.* **3**, 145 (2008).
29. E. Kluza *et al.*, *Nano Lett.* **10**, 52 (2010).
30. S. Hong *et al.*, *Chem. Biol.* **14**, 107 (2007).
31. J. Wang, S. M. Tian, R. A. Petros, M. E. Napier, J. M. Desimone, *J. Am. Chem. Soc.* **132**, 11306 (2010).
32. M. Shokeen *et al.*, *ACS Nano* **5**, 738 (2011).
33. D. R. Elias, A. Poloukhtine, V. Popik, A. Tsourkas, *Nanomed. Nanotechnol. Biol. Med.*, published online 11 June 2012 (10.1016/j.nano.2012.05.015).
34. H. Lee, H. Fonge, B. Hoang, R. M. Reilly, C. Allen, *Mol. Pharm.* **7**, 1195 (2010).
35. J. B. Haun, D. A. Hammer, *Langmuir* **24**, 8821 (2008).
36. R. K. Jain, T. Stylianopoulos, *Nat. Rev. Clin. Oncol.* **7**, 653 (2010).
37. T. T. Goodman, P. L. Olive, S. H. Pun, *Int. J. Nanomed.* **2**, 265 (2007).
38. T. T. Goodman, J. Y. Chen, K. Matveev, S. H. Pun, *Biotechnol. Bioeng.* **101**, 388 (2008).
39. H. Cabral *et al.*, *Nat. Nanotechnol.* **6**, 815 (2011).
40. K. N. Sugahara *et al.*, *Cancer Cell* **16**, 510 (2009).
41. V. R. Muzykantov *et al.*, *Proc. Natl. Acad. Sci. U.S.A.* **96**, 2379 (1999).
42. J. E. Schnitzer, P. Oh, E. Pinney, J. Allard, *J. Cell Biol.* **127**, 1217 (1994).
43. S. Bhattacharyya, R. Bhattacharya, S. Curley, M. A. McNiven, P. Mukherjee, *Proc. Natl. Acad. Sci. U.S.A.* **107**, 14541 (2010).
44. E. A. Simone, T. D. Dziubla, V. R. Muzykantov, *Expert Opin. Drug Deliv.* **5**, 1283 (2008).
45. E. S. Olson *et al.*, *Proc. Natl. Acad. Sci. U.S.A.* **107**, 4311 (2010).
46. S. H. Crayton, A. Tsourkas, *ACS Nano* **5**, 9592 (2011).
47. Y. K. Reshetnyak, O. A. Andreev, M. Segala, V. S. Markin, D. M. Engelman, *Proc. Natl. Acad. Sci. U.S.A.* **105**, 15340 (2008).
48. A. Davies, D. J. Lewis, S. P. Watson, S. G. Thomas, Z. Pikramenou, *Proc. Natl. Acad. Sci. U.S.A.* **109**, 1862 (2012).
49. Y. K. Reshetnyak *et al.*, *Mol. Imaging Biol.* **13**, 1146 (2011).
50. A. A. Kale, V. P. Torchilin, *Methods Mol. Biol.* **605**, 213 (2010).
51. B. Romberg, W. E. Hennink, G. Storm, *Pharm. Res.* **25**, 55 (2008).
52. C. Alexiou *et al.*, *Eur. Biophys. J.* **35**, 446 (2006).
53. D. K. Chatterjee, L. S. Fong, Y. Zhang, *Adv. Drug Deliv. Rev.* **60**, 1627 (2008).
54. S. Krishnan, P. Diagaradjane, S. H. Cho, *Int. J. Hyperthermia* **26**, 775 (2010).
55. Y. L. Luo, Y. S. Shiao, Y. F. Huang, *ACS Nano* **5**, 7796 (2011).
56. G. R. Reddy *et al.*, *Clin. Cancer Res.* **12**, 6677 (2006).
57. K. C. Briley-Saebo *et al.*, *Magn. Reson. Med.* **56**, 1336 (2006).
58. S. Santra *et al.*, *Adv. Mater.* **17**, 2165 (2005).
59. A. M. Morawski *et al.*, *Magn. Reson. Med.* **51**, 480 (2004).
60. Z. L. Cheng, D. L. J. Thorek, A. Tsourkas, *Angew. Chem. Int. Ed.* **49**, 346 (2010).
61. P. Zou *et al.*, *Mol. Pharm.* **7**, 1974 (2010).
62. T. Dutta, N. K. Jain, *Biochim. Biophys. Acta* **1770**, 681 (2007).
63. N. Nishiyama *et al.*, *Cancer Res.* **63**, 8977 (2003).
64. C. Sanson *et al.*, *J. Control. Release* **147**, 428 (2010).
65. J. O. Kim, A. V. Kabanov, T. K. Bronich, *J. Control. Release* **138**, 197 (2009).
66. Y. P. Li *et al.*, *J. Control. Release* **144**, 314 (2010).
67. W. C. Cole *et al.*, *J. Nucl. Med.* **28**, 83 (1987).
68. E. A. Simone *et al.*, *Biomaterials* **33**, 5406 (2012).
69. T. A. Elbayoumi, V. P. Torchilin, *Eur. J. Nucl. Med. Mol. Imaging* **33**, 1196 (2006).
70. A. Jordan *et al.*, *J. Neurooncol.* **78**, 7 (2006).
71. P. Huang *et al.*, *Biomaterials* **32**, 9796 (2011).
72. J. F. Lovell *et al.*, *Nat. Mater.* **10**, 324 (2011).
73. L. M. Fleck, *Hastings Cent. Rep.* **36**, 13 (2006).
74. D. L. J. Thorek, D. R. Elias, A. Tsourkas, *Mol. Imaging* **8**, 221 (2009).
75. N. Parker *et al.*, *Anal. Biochem.* **338**, 284 (2005).
76. P. Nair, *Curr. Sci.* **88**, 890 (2005).
77. R. S. Herbst, D. M. Shin, *Cancer* **94**, 1593 (2002).
78. M. F. Press, C. Cordon-Cardo, D. J. Slamon, *Oncogene* **5**, 953 (1990).
79. S. D. Sweat, A. Pacelli, G. P. Murphy, D. G. Bostwick, *Urology* **52**, 637 (1998).
80. C. Marchal *et al.*, *Histol. Histopathol.* **19**, 715 (2004).
81. G. Zhang *et al.*, *Proc. Natl. Acad. Sci. U.S.A.* **107**, 732 (2010).
82. K. C. Gatter, G. Brown, I. S. Trowbridge, R. E. Woolston, D. Y. Mason, *J. Clin. Pathol.* **36**, 539 (1983).
83. M. Prutki *et al.*, *Cancer Lett.* **238**, 188 (2006).
84. S. J. Gendler, *J. Mammary Gland Biol. Neoplasia* **6**, 339 (2001).
85. E. Lacunza *et al.*, *Cancer Genet. Cytogenet.* **201**, 102 (2010).
86. J. S. Desgrosellier, D. A. Cheresh, *Nat. Rev. Cancer* **10**, 9 (2010).
87. O. Barreiro *et al.*, *J. Cell Biol.* **157**, 1233 (2002).
88. D. Stefanou, A. Batistatou, E. Arkoumani, E. Ntzani, N. J. Agnantis, *Histol. Histopathol.* **19**, 37 (2004).
89. A. Nanda, B. St. Croix, *Curr. Opin. Oncol.* **16**, 44 (2004).
90. R. Opavsky *et al.*, *J. Biol. Chem.* **276**, 38795 (2001).
91. T. Bogenrieder *et al.*, *Prostate* **33**, 225 (1997).
92. H. Fujimura *et al.*, *Oncology* **58**, 342 (2000).
93. D. M. Nanus *et al.*, *Int. J. Oncol.* **13**, 261 (1998).
94. R. O. Schlingemann, E. Oosterwijk, P. Wesseling, F. J. Rietveld, D. J. Ruiter, *J. Pathol.* **179**, 436 (1996).
95. L. Bingle, N. J. Brown, C. E. Lewis, *J. Pathol.* **196**, 254 (2002).
96. M. Loeffler, J. A. Krüger, A. G. Niethammer, R. A. Reisfeld, *J. Clin. Invest.* **116**, 1955 (2006).
97. C. E. Lewis, M. De Palma, L. Naldini, *Cancer Res.* **67**, 8429 (2007).

Acknowledgments: This research was supported in part by the NIH National Institute of Biomedical Imaging and Bioengineering (NIBIB) grant R01-EB012065, National Cancer Institute R01-CA157766, NIBIB R21-EB013226, NIBIB R21-EB013754, and National Heart, Lung, and Blood Institute RO1 HL087036.

10.1126/science.1226338

Downloaded from www.sciencemag.org on December 20, 2012

REVIEW

Soft Matter Models of Developing Tissues and Tumors

David Gonzalez-Rodriguez,[1]* Karine Guevorkian,[2]* Stéphane Douezan,[3]* Françoise Brochard-Wyart[3]†

Analogies with inert soft condensed matter—such as viscoelastic liquids, pastes, foams, emulsions, colloids, and polymers—can be used to investigate the mechanical response of soft biological tissues to forces. A variety of experimental techniques and biophysical models have exploited these analogies allowing the quantitative characterization of the mechanical properties of model tissues, such as surface tension, elasticity, and viscosity. The framework of soft matter has been successful in explaining a number of dynamical tissue behaviors observed in physiology and development, such as cell sorting, tissue spreading, or the escape of individual cells from a tumor. However, living tissues also exhibit active responses, such as rigidity sensing or cell pulsation, that are absent in inert soft materials. The soft matter models reviewed here have provided valuable insight in understanding morphogenesis and cancer invasion and have set bases for using tissue engineering within medicine.

Soft tissues are complex deformable materials whose rheology is determined by dynamical fluctuations caused by cell activity. These characteristics of biological tissues make them akin to soft matter, a similarity that has been exploited to investigate tissue mechanics—that is, the movements and reshaping of tissues under the action of forces. The most fruitful analogy is that between tissues and liquids (*1*) with a viscoelastic rheology (*2*), but specific aspects of tissue behavior have also been explained by analogies with other soft materials, such as viscoelastic pastes (*3*), foams (*4*), emulsions (*5*), colloids (*6*), and polymers.

This article reviews recent work on the application of physical and soft matter concepts to understand how soft tissues respond to forces. We focus our discussion on soft tissues, such as early embryonic tissues or tumors, in which the expression of extracellular matrix molecules that rigidify the tissue is low. Such tissues are well modeled by cellular aggregates, a model system

[1]Laboratoire d'Hydrodynamique (LadHyX), CNRS UMR 7646, Ecole Polytechnique, 91128 Palaiseau, France. [2]Institut de Génétique et de Biologie Moléculaire et Cellulaire (IGBMC), CNRS UMR 7104 and INSERM U964, Université de Strasbourg, 67400 Illkirch, France. [3]Physico-Chimie Curie, Institut Curie, Université Pierre et Marie Curie and CNRS UMR 168, 26 rue d'Ulm, 75005 Paris, France.

*These authors contributed equally to this work.
†To whom correspondence should be addressed. E-mail: brochard@curie.fr

reviewed by Lin and Chang (*7*). We start by discussing the work of Malcolm Steinberg, who made the founding contribution to this research field by proposing the analogy between embryonic tissues and liquids (*1*, *8*). Similarities between tissues and liquids or other soft materials have proven fruitful to quantitatively characterize the rheology of tissues and to explain a number of dynamical tissue behaviors reminiscent of those observed in physiology and development, such as cell sorting or tissue spreading. In spite of the power of such analogies, living tissues additionally display active responses that are not observed in passive soft materials, such as rigidity sensing or cell pulsation. We end the Review by discussing how these advances in tissue mechanics are being applied to understand embryonic morphogenesis, identify determining factors in cancer propagation, and develop novel medical approaches that use tissue engineering.

Steinberg's Differential Adhesion Hypothesis

A liquid is formed by molecules that remain cohesive because of the existence of attractive forces at the molecular scale. At the macroscopic scale, a liquid behaves as a continuous medium, and molecular interactions manifest themselves as the liquid's mechanical properties, such as viscosity (the resistance of the liquid to deformation) and surface tension (the tendency of a liquid to minimize its total surface because of the unfavorable attractive force imbalance experienced by molecules at the liquid's surface). Similar to liquids consisting of molecules with attractive interactions, tissues consist of cells with adhesive interactions (mediated by cell adhesion molecules such as cadherins). Analogous to liquids, the individual size of a cell is much smaller than the typical size of a tissue. Thus, tissues can also be treated as continuous media and their rheology described by macroscopic properties such as surface tension and viscosity, which for tissues crucially depend on intercellular adhesion, among other parameters.

The idea of describing tissues as liquids was inspired by cell sorting experiments. While studying amphibian embryonic development, Holftreter observed an affinity of alike cells to sort out and associate themselves, which led him to introduce the concept of "tissue affinities" (*9*). In a seminal 1963 article, Steinberg proposed the Differential Adhesion Hypothesis (DAH) to explain the universal cell sorting behavior through an analogy with the behavior of liquids (*1*). If oil and water are mixed in a liquid droplet, the two liquid phases separate in order to minimize the total interfacial energy. Similarly, when two different types of cells are randomly mixed forming an aggregate, the two cell populations spontaneously sort out. The final equilibrium configuration minimizes the total surface energy and depends on the surface tensions of the cell populations and their interfacial tension (*10*). For an interfacial tension smaller than the difference of surface tensions of the two cell populations, one tissue engulfs the other, with cells having the larger surface tension occupying the interior of the mixed aggregate, whereas for larger interfacial tension, the engulfment is partial. Thus, cell sorting is driven by differences in tissue surface tensions, which are largely determined by differences in expression of cell adhesion molecules, as has been experimentally demonstrated (*11*, *12*). In an experiment on the role of cell adhesion in tissue surface tension, Foty and Steinberg (*12*) transfected otherwise identical mouse fibroblast cell lines to express different levels of N-, P-, or E-cadherins. The surface tension of aggregates of these cell lines was measured by parallel-plate compression. Independently of the cadherin type, tissue surface tension was found to be linearly proportional to the cadherin expression level. Moreover, cell sorting experiments using heterotypic aggregates of all combinations of the different cell lines systematically produced the cell sorting outcomes predicted by comparing the surface tensions of the different cell populations.

Steinberg's hypothesis that cell sorting in tissues arises from differences in surface tension between different cell populations has gathered extensive experimental support (*13*) and is now widely accepted. Although energy-minimizing surface tension appears to determine the equilibrium configuration of a tissue, cellular motility and the renewal of continuously bonding and dissociating adhesive junctions are required for a tissue to overcome local energy barriers and progress toward equilibrium. The DAH's postulate that tissue surface tension is determined by the level of expression of cell adhesion molecules remains disputed, and alternative hypotheses have been formulated. The Differential Surface Contraction Hypothesis (DSCH) (*14*) proposes that surface tension arises from differences in actomyosin-driven cell cortical contractility. In the original formulation of the DSCH proposed by Harris (*14*), cells with large contractility would strongly tend to minimize their exposed surface on a cell aggregate, thus exhibiting a large tissue surface tension. Exposure of the more contractile cells to the external medium would be very energetically unfavorable, with cell contractility being reduced on heterotypic cell interfaces and further reduced in homotypic cell contacts, thus explaining the spontaneous sorting of cell populations with different contractilities. Experiments of cell sorting in aggregates from different layers of the zebrafish gastrula have yielded partial support for the role of contracility in tissue surface tension. Schötz *et al*. determined that differential adhesion, which is dependent on E-cadherin expression, influences positioning between zebrafish germ layer tissues (*15*). Krieg *et al*. concluded that tissue surface tension correlated with cell cortical tension [as measured by atomic force microscopy (AFM)] but not with cadherin expression (*16*). A limitation of this conclusion arises from the use of AFM to measure cortical tension. AFM measures single-cell responses on time scales of the order of seconds, much smaller than the time scales relevant for tissue surface tension (typically hours), thus making a direct comparison between AFM-measured cortical tension and surface tension unclear. The Differential Interfacial Tension Hypothesis (DITH) (*17*) combines the DAH and the DSCH to propose that tissue self-arrangements are governed by differences in interfacial tensions, which depend both on cell adhesion and cell contractility. Consistent with this idea, Krieg *et al*. (*16*) and Manning *et al*. (*18*) postulated that tissue surface tension is in general determined by both intercellular adhesion and cell cortical tension. Intercellular adhesion increases tissue surface tension, whereas cortical tension does not necessarily increase tissue surface tension (as originally proposed by Harris), but rather it has competing effects on surface tension. This is so because cortical tension not only increases cell-medium tension (which increases tissue surface tension) but it also increases cell-cell tension (which reduces tissue surface tension). The roles of intercellular adhesion and cortical tension in regulating intercellular contacts remain a subject of current research. Maître *et al*. quantified cortex tension at the cell-cell interface by separating cell doublets using dual micropipette aspiration (*19*). Their results suggest that cortical tension dominates over adhesion in controlling interfacial tension and cell-cell contact expansion, whereas adhesion is needed to mechanically couple the cortices of adhering cells.

Characterization of the Mechanical Properties of Tissue

In order for the DAH to become quantitative, it was necessary to measure the mechanical parameters of tissues. Tissue surface tension is a key parameter to characterize long-term equilibrium conditions, and rheological parameters are required to characterize the dynamic evolution of a tissue under the action of forces. The choice of the appropriate rheological parameters depends on the physical model adopted to describe tissue behavior. Broad experimental evidence indicates that soft tissues behave as elastic solids at short time scales (seconds to minutes) because their short-term deformation is proportional to the applied load and the tissue quickly recovers its initial shape if the load is released. At longer time scales (minutes to hours), tissues undergo cellular reorganizations, which lead to more persistent deformations, usually described experimentally as a viscoelastic behavior (*2*, *20*, *21*). The existing experimental observations have lead to two paradigms to characterize tissue rheology. The first paradigm postulates that tissues behave as viscoelastic fluids with a surface tension (*2*, *20*, *21*), and thus a model tissue is characterized by its surface tension (γ), Young's modulus of elasticity (E), and dynamic viscosity (η) to capture that over long time scales, tissues flow as viscous

Downloaded from www.sciencemag.org on December 20, 2012

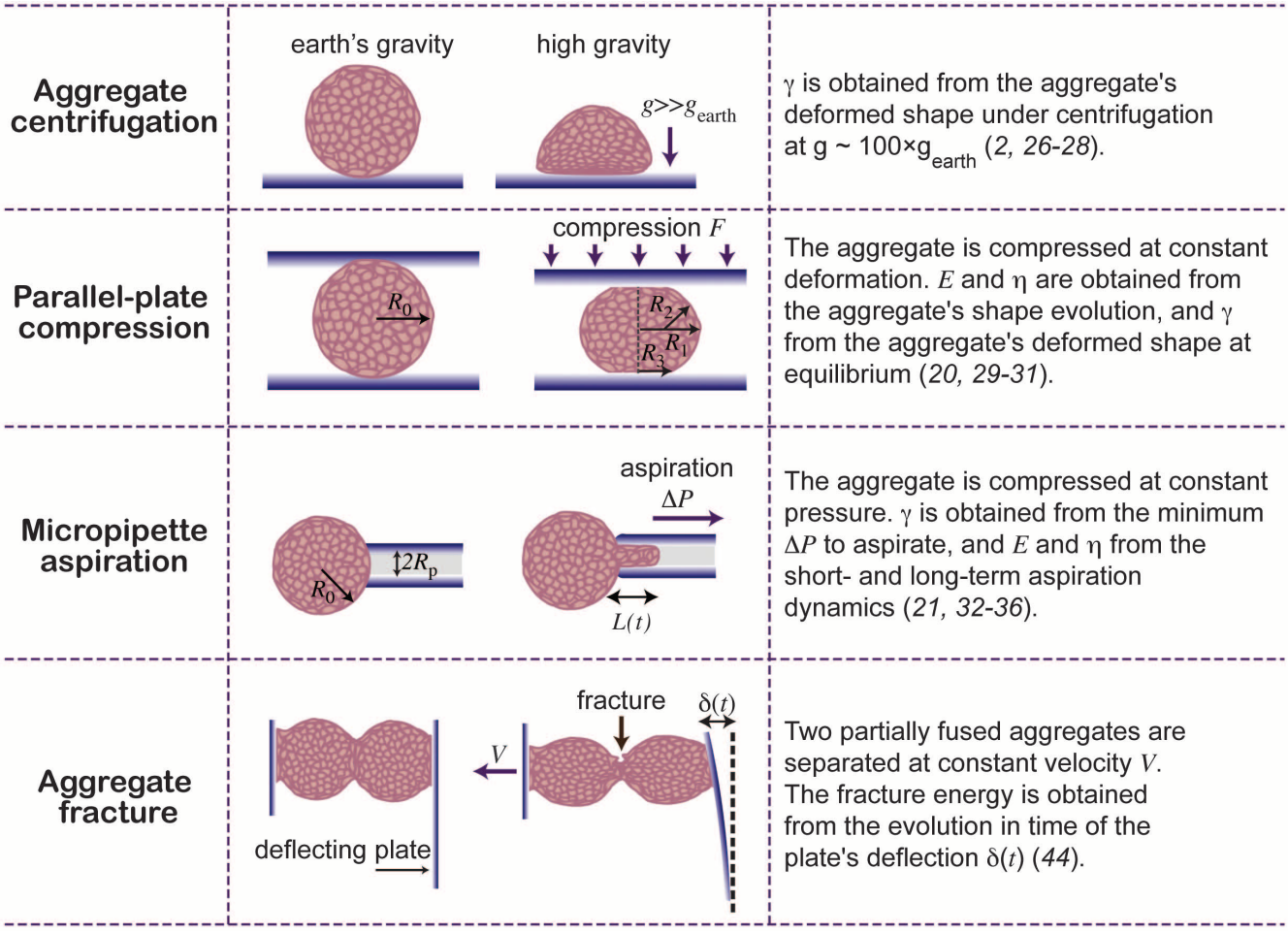

Fig. 1. Primary experimental techniques used to quantify mechanical properties of model tissues.

fluids. The second paradigm describes a tissue as an elasto-visco-plastic solid, characterized by a Young's modulus, a dynamic viscosity, and a yield stress (*22*–*24*). The yield stress is a threshold of stress below which the tissue can elastically recover its initial shape after the load is released. According to this second paradigm, if the applied stress is larger than the yield stress the tissue acquires permanent plastic deformations that remain present even after the load is released. In the following, we discuss the main techniques that have been developed to measure tissue mechanical parameters, which are illustrated in Fig. 1; some of these techniques have also been reviewed by Krens and Heisenberg (*25*).

Phillips and Steinberg proposed characterizing tissue surface tension by using aggregate centrifugation. It consists of subjecting the tissue to a centrifugal field that is a few hundred times stronger than gravity in order to produce measurable deformations (*26*). When an aggregate is centrifuged for a sufficiently long time, it adopts a flattened shape, which is independent of the initial aggregate shape. The degree of flattening is inversely correlated with the tissue surface tension. Later improvements of the technique have produced quantitative measurements of the tissue surface tension by using an analysis algorithm of the deformed aggregate shape (*27*, *28*). By following the evolution of the aggregate shape in the centrifugal field (*2*) or its shape relaxation after centrifugation is stopped, this technique could in principle be used to evaluate the tissue's elastic modulus and viscosity.

To date, the most widely used technique to characterize tissue properties has been parallel-plate compression, introduced by Steinberg and co-workers (*20*, *29*, *30*). In this method, an aggregate is placed between two nonadhering parallel plates and compressed to a fixed deformation. A scale measures the evolution of the compression force as a function of time, which allows the determination of the aggregate's viscoelastic properties (η, E). The aggregate eventually reaches an equilibrium shape, analogous to the shape of a liquid drop compressed between two plates. From knowledge of the equilibrium shape of the aggregate and of the corresponding applied force F, the aggregate surface tension can be determined as $\gamma = (1/R_1 + 1/R_2)^{-1}F/(\pi R_3^2)$, where R_1 and R_2 are the principal radii of curvature of the deformed aggregate and πR_3^2 is the contact area between the aggregate and either of the plates (Fig. 1) (*29*). The value of the surface tension is very sensitive to an accurate determination of the aggregate's equilibrium shape, which can be experimentally challenging (*31*).

Micropipette aspiration is a more recently introduced technique to characterize tissue rheology (*21*, *32*–*36*). In the method proposed by Guevorkian *et al.* (*21*), an aggregate is aspirated at constant suction pressure into a micropipette of smaller diameter than that of the aggregate, and the length of the aspirated tongue, $L(t)$, is tracked with time. For the aggregate to be aspirated, the applied suction pressure must be larger than a critical aspiration pressure ΔP_c, related to the aggregate's surface tension by $\gamma = (1/R_p - 1/R_0)^{-1}\Delta P_c/2$, where R_p and R_0 are the micropipette and aggregate radii, respectively. After aspirating the aggregate for a long enough time to capture its long-term behavior, the pressure is released, causing the aggregate to retract out of the pipette under the action of its surface tension. By fitting the aspiration and retraction curves

Downloaded from www.sciencemag.org on December 20, 2012

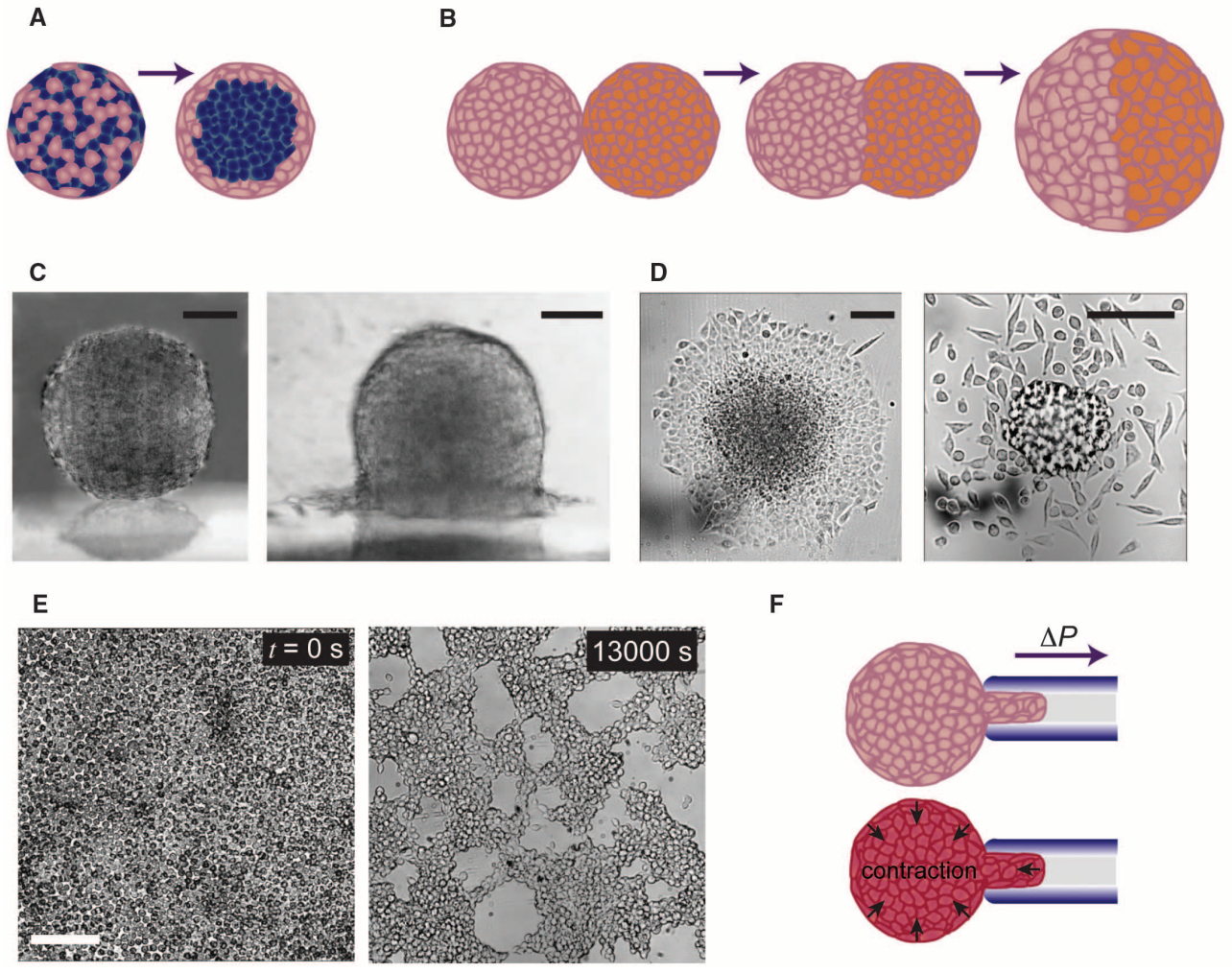

Fig. 2. Wetting analogies of tissue behavior. (**A**) Cell sorting. Two different cell populations (pink and blue) in a cell aggregate spontaneously sort out according to their surface and interfacial tensions. (**B**) Aggregate fusion. When brought into contact, two aggregates of the same cell line fuse to yield a larger, spherical aggregate. (**C**) Aggregate spreading on a wettable substrate. Reprinted with permission from (*57*). (**D**) Long-term spreading dynamics. As the aggregate cohesivity is decreased, the dynamics of the precursor film transitions from a liquid (left) to a 2D gas (right). Reprinted with permission from (*3*). (**E**) Dewetting of a cellular monolayer on a nonwettable substrate, a phenomenon opposite to spreading. Reprinted with kind permission of The European Physical Journal (EPJE) from (*6*). Scale bars, 100 μm. (**F**) Aggregate shivering. Active pulsatile contractions are observed during micropipette aspiration when the aspiration pressure is within a certain range.

to a viscoelastic model, the aggregate's elastic modulus, viscosity, and surface tension are determined. This technique has the advantage of a relatively simple experimental setup and image analysis. Using this technique on aggregates of mouse sarcoma cell lines expressing E-cadherin, Guevorkian *et al*. reported that the aggregate's surface tension increased with the applied pressure (*21*), which could indicate an active reinforcement of the aggregate in response to the applied stress. Such a reinforcement has not been reported in parallel-plate compression experiments. Although in parallel-plate compression aggregates are compressed to a constant strain, with the exerted stresses being relaxed over a typical time scale of about an hour, in micropipette aspiration aggregates undergo a continuous traction at constant stress. It has been reported that traction forces elicit active cell contractile responses (*37*, *38*), which may not arise during compression. A systematic study comparing parallel-plate compression and micropipette aspiration on aggregates of the same cell lines would help to clarify the effect of these differences. It has also been pointed out that whereas in parallel-plate compression the whole aggregate is stressed, micropipette aspiration probes only a subset of the aggregate's cells (*39*). The number of cells subjected to stress scales as R_p^3. Thus, for the continuum hypothesis to be valid and the technique applicable to characterize aggregate rheology, the micropipette radius should be large enough to probe a few hundreds of cells, which is usually accomplished with $R_p \approx 30$ μm.

The existence of a yield modulus above which aggregates exhibit plastic behavior remains a matter of controversy. Some authors have postulated the existence of a yield modulus in tissues, which physically would arise from the critical force required to break intercellular bonds and induce cellular reorganization (*22*). To our knowledge, no systematic experimental investigation of the existence of a yield stress in tissues has been conducted. Existing experimental observations such as the spontaneous fusion of two aggregates (*40*) seem to suggest that the yield stress, if it exists, is smaller than the stresses induced by tissue surface tension, and thus deformations are relaxed by surface tension over a time scale of the order of $\eta R/\gamma$, where R is the characteristic aggregate size (typically a few hundred micrometers). Moreover, bond formation and dissociation is more accurately described as a dynamic process, where the formation and dissociation rates vary continuously with the applied load. An appealing solution to the debate about the existence of tissue plasticity has been suggested by Marmottant *et al*. (*41*), who proposed that the

Downloaded from www.sciencemag.org on December 20, 2012

rheological description of tissue behavior depends on the time scale considered. When the applied stress is larger than the typical energy barrier for cell rearrangement, stresses are relaxed fast. When the residual stresses become small compared with energy barriers, they are relaxed by fluctuations only, and thus stress relaxation substantially slows down. In short-time observations, residual stresses can be described as tissue plasticity, even if they are eventually relaxed at long enough times. Depending on the cell line, the time for complete stress relaxation may be minutes, hours, or even days. Accurate measurement of tissue surface tension by parallel-plate compression, which assumes that equilibrium conditions have been attained, requires that the time allowed for tissue relaxation is long enough to completely dissipate residual stresses (*41*). A definitive answer to the debate of characterizing tissues as either viscoelastic fluids or visco-elasto-plastic solids could come from measuring the frequency response of tissues to a periodic forcing, a much-needed experiment that to our knowledge has not previously been reported. Different constitutive models (such as the viscoelastic Maxwell model, the generalized viscoelastic Kelvin model, or the elasto-plastic Bingham fluid) predict different frequency responses. Thus, periodic forcing experiments could be used to determine the appropriate constitutive model for soft tissues and whether the same constitutive model with different parameter values can describe different types of tissue, or rather whether different models are needed for different tissues.

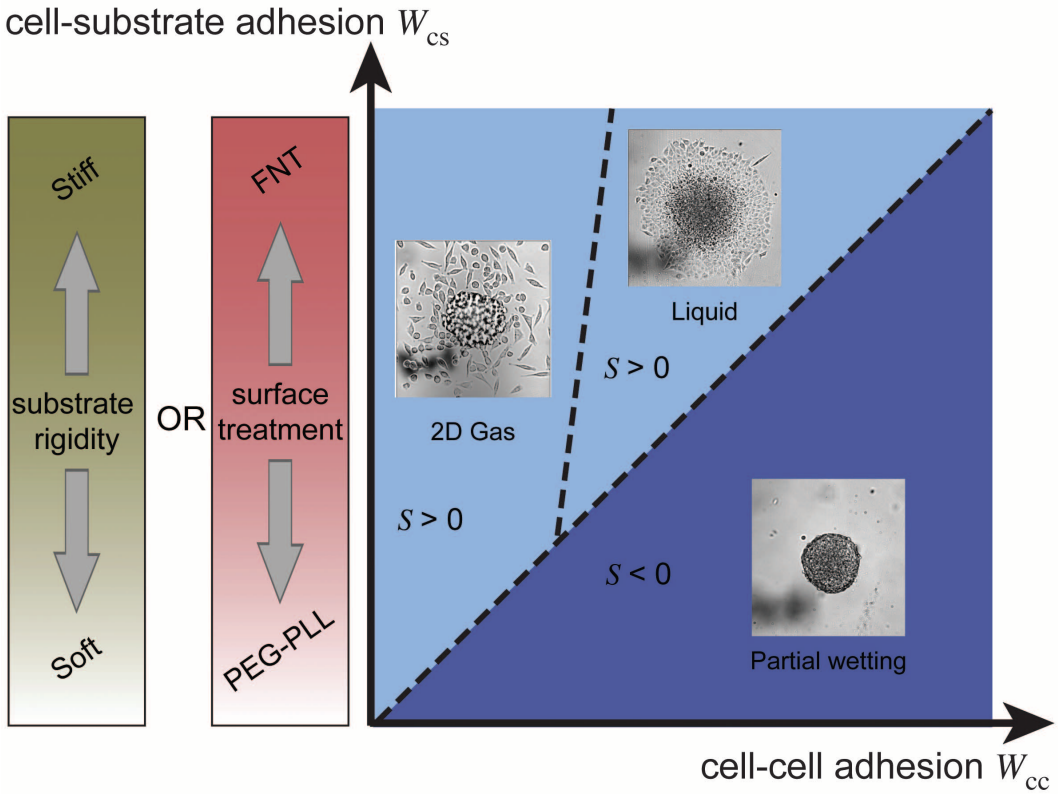

Fig. 3. Phase diagram of tissue spreading. The aggregate's fate is governed by a competition between the cell-substrate adhesion energy W_{cs} and the cell-cell adhesion energy W_{cc}, the difference of which sets the sign of the spreading parameter $S = W_{cs} - W_{cc}$. The images show the long-term fate of the aggregate in each of the regions. The cell-substrate energy W_{cs} can be controlled either by modifying the substrate's surface chemistry [nonadhesive PEG-poly-L-lysine (PEG-PLL) versus adhesive fibronectin (FNT)] or its rigidity (soft versus stiff). The two top images are reprinted with permission from (*3*).

At time scales comparable with the time for cell division (usually of the order of a day), cell proliferation and apoptosis affect aggregate rheology. A theoretical model by Ranft *et al.* (*42*) suggests that cell rearrangements induced by cell division and apoptosis will result in a viscous tissue response, independent of the adhesion-mediated viscosity. At long time scales, both components of tissue viscosity must be accounted for. Moreover, unlike adhesion-mediated viscosity, proliferation-controlled viscosity is affected by the isotropic pressure applied on the cells because high pressures have experimentally been shown to inhibit cell proliferation (*43*).

Last, another type of experimental technique characterizes the resistance of a model tissue to stress-induced failure, either by internal fracture (*44*) or by detachment from a substrate modeling the extracellular matrix. By pulling apart two partially fused aggregates at constant speed and measuring the fracture energy, recent experiments in our laboratory suggest an analogy between tissues and polymers. Similar to polymers, the resistance of tissues to fracture appears to depend on the imposed deformation rate.

Wetting Analogies of Tissue Behavior

Analogies between tissue mechanics and dynamical phenomena involving liquid interfaces, known as wetting phenomena, have been used to explain several ubiquitous tissue behaviors. Among such behaviors, cell sorting (illustrated in Fig. 2A) has received substantial attention because it is a model phenomenon for the mutual envelopment of different tissue layers during morphogenesis (*1*). Graner and Glazier (*45*, *46*) developed a two-dimensional (2D) cellular Potts model to investigate the physics of cell sorting. By accounting for differential adhesion and for random cell fluctuations associated with cell activity, their model was able to reproduce cell sorting. The model predicts the existence of two regimes in the evolution of an aggregate formed by two randomly mixed cell populations. The fast, short-time regime leads to a partial cell sorting state, whereas the slower, long-time regime leads to complete cell sorting. Both the partial and complete cell sorting states have been observed experimentally.

The tendency of cellular aggregates to spontaneously round up and acquire a spherical shape, which is an effect of the area-minimizing surface tension, is analogous to the behavior of liquid drops. The dynamics of rounding up have been experimentally studied in 2D hydra aggregates, which spontaneously evolve from an elliptic to a circular shape (*47*), and in 3D chick embryo aggregates, which evolve from an irregular to a spherical shape (*48*). Both phenomena are reasonably well described by modeling an aggregate as a viscoelastic liquid drop with a surface tension.

Fusion of two cell aggregates (Fig. 2B) is analogous to the coalescence of two viscous liquid drops. The dynamics of spontaneous aggregate fusion (*40*, *49*) are well described by a balance between the energy gain by reducing the surface area, which is driven by surface tension, and the energy dissipation due to internal viscous friction. Tissue phenomena governed by a balance between surface tension (γ) and viscosity (η), such as tissue envelopment, rounding up,

Downloaded from www.sciencemag.org on December 20, 2012

or fusion, are completed over a characteristic time scale given by $R\eta/\gamma$, where R is the final aggregate radius and γ/η is a typical velocity of the order of 10^{-8} m/s, which yields a typical time scale of several hours.

A striking analogy between tissue mechanics and liquid wetting is found in tissue spreading (Fig. 2C) (*3*, *50*). As with liquid wetting, the aggregate's fate is determined by the sign of the spreading parameter $S = W_{cs} - W_{cc}$, where W_{cs} and W_{cc} are the cell-substrate and cell-cell adhesion energies per unit area, respectively. These adhesion energies are closely related to surface and interfacial tensions ($W_{cc} = 2\gamma$ and $W_{cs} = \gamma_{sm} + \gamma - \gamma_{cs}$, with γ_{cs}, γ_{sm}, and $\gamma = \gamma_{cm}$ being the cell-substrate, substrate-medium, and cell-medium interfacial tensions, respectively). The analogy between tissue spreading and liquid wetting is most remarkable because cells use distinct machineries to adhere to one another (typically involving cadherin pathways) and to adhere to substrates (typically involving integrins). This is in contrast to inert soft matter wetting systems, in which surface energies are all driven by the same physics of molecular interactions. Although this wetting analogy is supported by experimental evidence, there could be some tissue types with strong feedback between cadherin and integrin pathways in which the analogy breaks down or the wetting behavior changes as a function of time. The effect of varying cell-cell and cell-substrate adhesion energy on aggregate spreading is illustrated in Fig. 3. If $S < 0$, the cell-cell adhesion energy is larger than the cell-substrate adhesion energy. This is a nonwettable surface on which the aggregate remains spherical, a state termed "partial wetting" because the aggregate exhibits a finite contact angle with the surface. Partial wetting is experimentally observed when a cell aggregate is placed on a polyethylene glycol (PEG)–coated substrate. In contrast, if $S > 0$, cell-substrate contact is energetically favorable, and the aggregate spreads on the surface, such as when a cell aggregate is placed on a fibronectin-coated substrate. The dynamical laws governing aggregate spreading are the same as for a viscoelastic paste (*3*). At long times (Fig. 2D), a striking new analogy to liquid wetting is observed (*3*): A precursor film of cells spreads around the aggregate. In strongly cohesive aggregates (large W_{cc}), the film is a continuous cellular monolayer, whereas in weakly cohesive aggregates individual cells can escape from the aggregate. This is reminiscent of a wetting transition from a liquid to a 2D gas. By using aggregates of mouse sarcoma cell lines expressing different E-cadherin levels, Douezan *et al*. (*3*) demonstrated that this liquid-to-gas transition in aggregates is induced by reducing cadherin expression. This suggests that the epithelial-mesenchymal transition, which is associated with a reduction of cadherin expression and plays important roles in embryonic development and tumor metastasis, may be interpreted as a wetting transition. Moreover, knowledge of the dynamical laws governing tissue spreading allows to quantitatively characterize the action of drugs in inhibiting the spreading of tumors (*51*).

When a liquid film is placed on a nonwettable substrate, it retracts from the substrate by breaking down into isolated drops, such as occurs to the water film on one's skin when coming out of the shower. This phenomenon, called dewetting, has also been observed in cellular systems (*6*, *52*). When a confluent layer of cells is placed on a PEG-coated substrate, the cells spontaneously withdraw from the surface to form isolated aggregates, following the same dynamical law as viscous liquid dewetting (Fig. 2E) (*6*). If initially the cells are subconfluent, they migrate on the surface following collectively a diffusive law. The cells eventually meet and form 3D aggregates, according to the same dynamical law as the diffusion-limited aggregation of colloids (*49*).

Mechanotransduction in Tissue Mechanics

Because tissues are composed of living cells capable of sensing and reacting to forces, they exhibit active mechanotransduction phenomena that distinguish them from passive materials. An important example of this active behavior is the ability of tissues to sense and react to substrate rigidity. As the substrate becomes stiffer, cells show increased contractile traction forces, more stable focal adhesions, better defined actin stress fibers, and increased adhesion strength (*53*–*56*). In terms of the wetting analogy of tissue spreading discussed above, as the substrate becomes stiffer, cell-substrate adhesion becomes more favorable, and W_{cs} increases (Fig. 3). It has been experimentally shown that the rigidity of the substrate can induce a wetting transition from partial wetting ($S < 0$) below a threshold of substrate rigidity (E_c) to complete wetting ($S > 0$) above this rigidity threshold (*57*). Unlike the statics of passive liquid wetting, which are only affected by substrate rigidity if the substrate is deformable enough to form a wetting ridge around the liquid drop (*58*), the rigidity-induced wetting transition in cellular aggregates is observed without appreciable deformation of the substrate. The dynamics of spreading and cell diffusion from the aggregate are also affected by substrate rigidity. On a substrate rigid enough to induce complete wetting, the long-term spreading dynamics follows a diffusive law with a diffusion coefficient that depends on the rigidity, with a maximum for $E \approx 2E_c$ (*57*). If the experiment starts from a cell layer spread on a soft substrate, cells dewet the substrate and form 3D aggregates, whereas on a rigid substrate, cells do not aggregate (*6*, *59*). This rigidity-dependent wetting suggests a physical explanation of why cancer invasion is stimulated by increased connective tissue stiffness, an effect known as desmoplasia and observed, for example, in breast cancer and pancreatic adenocarcinoma (*59*).

Tissue pulsation is another active phenomenon that plays important roles in embryonic development (*60*). When a cellular aggregate is aspirated into a micropipette within a precise range of aspiration pressures, pulsatile tissue contractions are observed, a phenomenon that has been termed "aggregate shivering" (Fig. 2F) (*38*). Aggregate shivering has also been observed when an aggregate is stretched between two plates but not in parallel-plate compression. Shivering has been explained as an active contraction of the cells in the aggregate after they have been stretched beyond a certain threshold. The existence of a time delay between stretching and active cell contractile response quantitatively explains the characteristic time between shivering contractions (*38*) as well as the pulsation of amnioserosa cells observed during dorsal closure in the embryonic development of *Drosophila* (*61*).

Another active response of tissues to forces is the hyperrestoration principle proposed by Beloussov *et al*. (*62*). This principle conjectures that when a cell or tissue is shifted from its mechanical equilibrium by an external force, it develops an active response directed toward restoration of the initial condition. However, the restorative response generally overshoots the mere compensation of the effect caused by the external force (hyperrestoration). Beloussov and Luchinskaia experimentally illustrated this principle by stretching *Xenopus* tissue explants (*63*). They reported that, once the stretching force ceases, the tissue, instead of simply relaxing forces, continues elongating and exhibits an extensive shape reorganization.

Applications to Physiology and Bioengineering

The knowledge in tissue mechanics gained through analogies with soft matter has been applied to understand important phenomena in physiology. For example, Winters *et al*. showed an inverse correlation between the surface tension of a tumor and its invasive potential (*64*). They determined the in vitro surface tension of malignant astrocytoma cell lines by using the parallel-plate compression technique and their cell invasiveness by using a matrigel transfilter invasion assay. They found that the relevant parameter to determine tumor invasiveness is the surface tension and not simply cadherin expression. In their experiments, surface tension did not correlate with the N-cadherin expression level, which they attribute to an effect on surface tension of cell interaction with the extracellular matrix. The effect of extracellular matrix interactions on tumor progression was further investigated by Hegedus *et al*. (*65*), who showed that tumor-invasive patterns depend on a balance between cell-cell interactions (mediated by cadherins) and cell-matrix interactions (mediated by integrins as well as by metalloprotease activity), and also by Sabari *et al*. (*51*), who showed that assembly of a fibronectin

Downloaded from www.sciencemag.org on December 20, 2012

extracellular matrix slows down or suppresses spreading of an aggregate of brain tumor cells.

Tissue wetting analogies have broad implications to embryonic development. Cell sorting plays a role in zebrafish and *Xenopus* gastrulation, mouse blastocyst formation, or chick limb bud formation, as reviewed by Krens and Heisenberg (*25*). Although the direct applicability of in vitro cell sorting behaviors to explain embryonic tissue layering remains debated (*66*), sorting patterns of embryonic tissues observed in vivo can often be reproduced in vitro by using cellular aggregates, as demonstrated, for example, with the organization of brain cortical layers in mice (*67*). Aggregate fusion is found, for example, in early chick heart development, in which septa and valves form by fusion of endocardic swellings known as cardiac cushions (*40*). Viscous tissue spreading is a phenomenon ubiquituosly found in morphogenesis whenever tissue layers rearrange their relative positions, such as during embryonic epiboly (*68*). The power of analogies to liquid systems is not restricted to 3D geometries. In the 2D cell patterning observed in the retinal epithelium of *Drosophila* (*4*, *69*), cone cells arrange themselves following the same energy-minimization principles that govern the organization of soap bubbles in a 2D liquid film. Similarly, the evolution of the configurational pattern of cells forming the wing disc epithelial layer in *Drosophila* can be explained by global energy minimization of a system governed by the interaction between line tension, cell elasticity, and cell contractility (*70*).

Understanding tissue mechanics provides the basis to tissue engineering, which aims to develop new strategies of medical treatment based on artificial tissue regeneration. In building artificial tissues, surface tension can be used to induce the spontaneous assembly and organization of cells in analogous configurations as those found in vivo. This is exemplified by the spontaneous in vitro self-assembly of pancreatic islet cells, which are capable of reproducing a realistic islet topology (*71*). Using surface tension to induce self-organization is one of the bases of the bioprinting techniques developed by Forgacs and co-workers (*72*). In contrast with traditional tissue engineering methods, which propose the implantation of a tissue scaffold seeded with cells, bioprinting is a scaffold-free approach that uses the liquid-like fusion and wetting properties of cellular aggregates to form organized 3D tissue structures. Closely placed aggregates fuse and form larger structures, whereas undesired aggregate spreading is prevented by the use of nonwettable substrates (*73*, *74*). Forgacs and co-workers have developed two different bioprinting approaches to produce 3D structures. In the first approach, a modified inkjet printer uses cellular aggregates as "ink drops" and deposits them layer by layer with collagen sheets as support. Then, spontaneous fusion of the cell aggregate ink drops produces 3D tissue structures (*74*). The second approach, devised for the assembly of long structures such as blood vessels, uses the inkjet printer to assemble the aggregates into 1D cylinders, corresponding, for example, to one longitudinal section of the vessel wall. These cell cylinders are appropriately placed in 3D space with the help of cylinders of agarose, a nonwettable biocompatible material, which eventually are removed to produce void spaces such as the vessel lumen (*75*). An alternative technique to assemble blood vessels has been proposed by Fleming *et al*. (*76*). This technique uses uniluminal spheroids, which are shell-like aggregate structures formed by an outer layer of smooth muscle cells, an inner layer of endothelial cells, and an internal space void of cells. Fusion of uniluminal spheroids yields elongated vessel-like tubes, a process that can be applied to engineer blood vessels.

In conclusion, soft matter physics has been fruitfully applied to quantitatively explain fundamental phenomena in tissue mechanics, such as cell sorting or tissue spreading. These advances in our fundamental knowledge of tissue mechanics are being applied to understand embryonic morphogenesis and cancer progression, and they are playing a crucial role in the development of the new field of tissue engineering. Several key questions in the field remain open. The rheology of soft tissues has not been conclusively described; in particular, the concept of tissue plasticity remains debated. Future experiments that allow discrimination between different constitutive models should be designed, such as investigations of the frequency response of tissues to forces. More generally, models of tissue mechanics have often focused on partial descriptions of tissue behavior that are successful in explaining specific features of a type of tissue at a certain scale. Future modeling efforts should discuss the general applicability of theoretical models to different tissues, as well as link the physics at different scales to provide a comprehensive view of tissue mechanics. Specifically, future studies should address how the macroscopically measurable tissue viscosity arises from and depends on biomolecular mechanisms, an important question that remains largely unexplored. A promising area of further applicability of soft matter concepts is the study of instabilities in which tissue surface tension plays a role, such as in epithelial dysplasia or cancerous invasion (*77*). Last, new and rapidly developing 3D cell culture techniques provide novel in vitro systems in which to study tissue mechanics. The closer proximity of these systems to in vivo conditions will help bridge existing gaps between observed in vitro behaviors and physiological phenomena.

References and Notes

1. M. S. Steinberg, *Science* **141**, 401 (1963).
2. H. M. Phillips, M. S. Steinberg, *J. Cell Sci.* **30**, 1 (1978).
3. S. Douezan *et al*., *Proc. Natl. Acad. Sci. U.S.A.* **108**, 7315 (2011).
4. T. Hayashi, R. W. Carthew, *Nature* **431**, 647 (2004).
5. L. L. Pontani, I. Jorjadze, V. Viasnoff, J. Brujic, *Proc. Natl. Acad. Sci. U.S.A.* **109**, 9839 (2012).
6. S. Douezan, F. Brochard-Wyart, *Eur. Phys. J. E* **35**, 34 (2012).
7. R.-Z. Lin, H.-Y. Chang, *Biotechnol. J.* **3**, 1172 (2008).
8. M. S. Steinberg, *Dev. Biol.* **180**, 377 (1996).
9. J. Holftreter, *J. Exp. Zool.* **94**, 261 (1943).
10. R. A. Foty, M. S. Steinberg, *Int. J. Dev. Biol.* **48**, 397 (2004).
11. D. Duguay, R. A. Foty, M. S. Steinberg, *Dev. Biol.* **253**, 309 (2003).
12. R. A. Foty, M. S. Steinberg, *Dev. Biol.* **278**, 255 (2005).
13. M. S. Steinberg, *Curr. Opin. Genet. Dev.* **17**, 281 (2007).
14. A. K. Harris, *J. Theor. Biol.* **61**, 267 (1976).
15. E.-M. Schötz *et al*., *HFSP J.* **2**, 42 (2008).
16. M. Krieg *et al*., *Nat. Cell Biol.* **10**, 429 (2008).
17. G. W. Brodland, *J. Biomech. Eng.* **124**, 188 (2002).
18. M. L. Manning, R. A. Foty, M. S. Steinberg, E.-M. Schoetz, *Proc. Natl. Acad. Sci. U.S.A.* **107**, 12517 (2010).
19. J.-L. Maître *et al*., *Science* **338**, 253 (2012).
20. G. Forgacs, R. A. Foty, Y. Shafrir, M. S. Steinberg, *Biophys. J.* **74**, 2227 (1998).
21. K. Guevorkian, M.-J. Colbert, M. Durth, S. Dufour, F. Brochard-Wyart, *Phys. Rev. Lett.* **104**, 218101 (2010).
22. D. Ambrosi, L. Preziosi, *Biomech. Model. Mechanobiol.* **8**, 397 (2009).
23. L. Preziosi, D. Ambrosi, C. Verdier, *J. Theor. Biol.* **262**, 35 (2010).
24. C. Giverso, L. Preziosi, *Math. Med. Biol.* **29**, 181 (2012).
25. S. F. G. Krens, C.-P. Heisenberg, *Curr. Top. Dev. Biol.* **95**, 189 (2011).
26. H. M. Phillips, M. S. Steinberg, *Proc. Natl. Acad. Sci. U.S.A.* **64**, 121 (1969).
27. H. Ninomiya, R. Winklbauer, *Nature* **10**, 61 (2008).
28. A. Kalantarian *et al*., *Biophys. J.* **96**, 1606 (2009).
29. R. A. Foty, G. Forgacs, C. M. Pfleger, M. S. Steinberg, *Phys. Rev. Lett.* **72**, 2298 (1994).
30. R. A. Foty, C. M. Pfleger, G. Forgacs, M. S. Steinberg, *Development* **122**, 1611 (1996).
31. A. Mgharbel, H. Delanoë-Ayari, J.-P. Rieu, *HFSP J.* **3**, 213 (2009).
32. J. T. Butcher, T. C. McQuinn, D. Sedmera, D. Turner, R. R. Markwald, *Circ. Res.* **100**, 1503 (2007).
33. M. von Dassow, L. A. Davidson, *Dev. Dyn.* **238**, 2 (2009).
34. M. von Dassow, J. A. Strother, L. A. Davidson, *PLoS ONE* **5**, e15359 (2010).
35. A. N. Mansurov, L. V. Beloussov, *Russ. J. Dev. Biol.* **42**, 101 (2011).
36. M. Durth, thesis, Ecole Polytechnique, France, and University of Seville, Spain (2012).
37. A. Micoulet, J. P. Spatz, A. Ott, *ChemPhysChem* **6**, 663 (2005).
38. K. Guevorkian, D. Gonzalez-Rodriguez, C. Carlier, S. Dufour, F. Brochard-Wyart, *Proc. Natl. Acad. Sci. U.S.A.* **108**, 13387 (2011).
39. G. Forgacs, I. Kosztin, *Physics* **3**, 43 (2010).
40. K. Jakab *et al*., *Dev. Dyn.* **237**, 2438 (2008).
41. P. Marmottant *et al*., *Proc. Natl. Acad. Sci. U.S.A.* **106**, 17271 (2009).
42. J. Ranft *et al*., *Proc. Natl. Acad. Sci. U.S.A.* **107**, 20863 (2010).
43. F. Montel *et al*., *Phys. Rev. Lett.* **107**, 188102 (2011).
44. C. Wiebe, G. W. Brodland, *J. Biomech.* **38**, 2087 (2005).
45. F. Graner, J. A. Glazier, *Phys. Rev. Lett.* **69**, 2013 (1992).
46. J. A. Glazier, F. Graner, *Phys. Rev. E Stat. Phys. Plasmas Fluids Relat. Interdiscip. Topics* **47**, 2128 (1993).
47. J.-P. Rieu, Y. Sawada, *Eur. Phys. J. B* **27**, 167 (2002).
48. J. C. M. Mombach *et al*., *Physica A* **352**, 525 (2005).
49. S. Douezan, F. Brochard-Wyart, *Soft Matter* **8**, 784 (2012).
50. P. L. Ryan, R. A. Foty, J. Kohn, M. S. Steinberg, *Proc. Natl. Acad. Sci. U.S.A.* **98**, 4323 (2001).
51. J. Sabari *et al*., *PLoS ONE* **6**, e24810 (2011).
52. D. Gonzalez-Rodriguez *et al*., *Phys. Rev. Lett.* **108**, 218105 (2012).
53. N. Q. Balaban *et al*., *Nat. Cell Biol.* **3**, 466 (2001).
54. D. E. Discher, P. Janmey, Y. L. Wang, *Science* **310**, 1139 (2005).
55. A. Nicolas, A. Besser, S. A. Safran, *Biophys. J.* **95**, 527 (2008).

Downloaded from www.sciencemag.org on December 20, 2012

56. L. Trichet *et al.*, *Proc. Natl. Acad. Sci. U.S.A.* **109**, 6933 (2012).
57. S. Douezan, J. Dumond, F. Brochard-Wyart, *Soft Matter* **8**, 4578 (2012).
58. M. E. R. Shanahan, *J. Phys. D Appl. Phys.* **20**, 945 (1987).
59. W. H. Guo, M. T. Frey, N. A. Burnham, Y. L. Wang, *Biophys. J.* **90**, 2213 (2006).
60. A. C. Martin, *Dev. Biol.* **341**, 114 (2010).
61. J. Solon, A. Kaya-Copur, J. Colombelli, D. Brunner, *Cell* **137**, 1331 (2009).
62. L. V. Beloussov, S. V. Saveliev, I. I. Naumidi, V. V. Novoselov, *Int. Rev. Cytol.* **150**, 1 (1994).
63. L. V. Beloussov, N. N. Luchinskaia, *Biochem. Cell Biol.* **73**, 555 (1995).
64. B. S. Winters, S. R. Shepard, R. A. Foty, *Int. J. Cancer* **114**, 371 (2005).
65. B. Hegedüs, F. Marga, K. Jakab, K. L. Sharpe-Timms, G. Forgacs, *Biophys. J.* **91**, 2708 (2006).
66. H. Ninomiya *et al.*, *J. Cell Sci.* **125**, 1877 (2012).
67. M. Ogawa *et al.*, *Neuron* **14**, 899 (1995).
68. O. Luu, R. David, H. Ninomiya, R. Winklbauer, *Proc. Natl. Acad. Sci. U.S.A.* **108**, 4000 (2011).
69. J. Käfer, T. Hayashi, A. F. M. Marée, R. W. Carthew, F. Graner, *Proc. Natl. Acad. Sci. U.S.A.* **104**, 18549 (2007).
70. R. Farhadifar, J.-C. Röper, B. Aigouy, S. Eaton, F. Jülicher, *Curr. Biol.* **17**, 2095 (2007).
71. D. Jia, D. Dajusta, R. A. Foty, *Dev. Dyn.* **236**, 2039 (2007).
72. V. Mironov *et al.*, *Biomaterials* **30**, 2164 (2009).
73. K. Jakab, A. Neagu, V. Mironov, R. R. Markwald, G. Forgacs, *Proc. Natl. Acad. Sci. U.S.A.* **101**, 2864 (2004).
74. K. Jakab *et al.*, *Tissue Eng. A* **14**, 413 (2008).
75. C. Norotte, F. S. Marga, L. E. Niklason, G. Forgacs, *Biomaterials* **30**, 5910 (2009).
76. P. A. Fleming *et al.*, *Dev. Dyn.* **239**, 398 (2010).
77. M. Basan, J.-F. Joanny, J. Prost, T. Risler, *Phys. Rev. Lett.* **106**, 158101 (2011).

Acknowledgments: We thank four anonymous reviewers for their valuable contributions. The authors declare no conflicts of interest.

10.1126/science.1226418

REVIEW

Unlike Bone, Cartilage Regeneration Remains Elusive

Daniel J. Huey, Jerry C. Hu, Kyriacos A. Athanasiou*

Articular cartilage was predicted to be one of the first tissues to successfully be regenerated, but this proved incorrect. In contrast, bone (but also vasculature and cardiac tissues) has seen numerous successful reparative approaches, despite consisting of multiple cell and tissue types and, thus, possessing more complex design requirements. Here, we use bone-regeneration successes to highlight cartilage-regeneration challenges: such as selecting appropriate cell sources and scaffolds, creating biomechanically suitable tissues, and integrating to native tissue. We also discuss technologies that can address the hurdles of engineering a tissue possessing mechanical properties that are unmatched in human-made materials and functioning in environments unfavorable to neotissue growth.

Nearly two decades ago, the concept of tissue engineering promised healing of damaged tissues and organs via the use of living, functional constructs. By manipulating cells, scaffolds, and stimuli, the premise was that tissues could be generated that, upon implantation, would integrate to native tissues and restore functions lost due to trauma, disease, or aging (*1*). Tissue engineers recognized that the first targets would be tissues with homogeneous structure and few cell types (*2*). Due to diffusion limitations, it was also anticipated that these would be thin, avascular tissues. Thus, the first cell-based products would be for skin and articular cartilage due to their almost two-dimensional nature. However, despite its more complex composition, including the presence of multiple cell types and vascularity, bone exhibits a high level of innate repair capability that is not present in cartilage. Hence, bone tissue, rather than cartilage, has seen more development as a target for regeneration.

Articular cartilage is the elegantly organized tissue that allows for smooth motion in diarthrodial joints. Our bodies possess a number of distinct cartilages: the hyaline cartilages of the nasal septum, tracheal rings, and ribs; the elastic cartilages of the ear and epiglottis; and the fibrocartilages of the intervertebral discs, temporomandibular joint disc, and knee meniscus. Articular cartilage is distinct in its weight-bearing and low-friction capabilities. Damage to this tissue can impair joint function, leading to disability. Unlike the majority of tissues, articular cartilage is avascular. Without access to abundant nutrients or circulating progenitor cells and by possessing a nearly acellular nature, cartilage lacks innate abilities to mount a sufficient healing response (Fig. 1). Thus, damaged tissue is not replaced with functional tissue, requiring surgical intervention (*3*). Traditional techniques for cartilage repair include marrow stimulation, allografts, and autografts (Fig. 2). Although successful in some aspects, each of these techniques has limitations. Marrow stimulation results in fibrocartilage of inferior quality that does not persist; allografts suffer from lack of integration, loss of cell viability due to graft storage, and concerns of disease transmission; and autografts also lack integration and require additional defects (*3*).

Limitations of Making an Engineered Cartilage for Clinical Use

For load-bearing tissues, correlations between structure and function must be understood to establish tissue engineering design criteria. Cartilage's viscoelastic properties manifest from its extracellular matrix (ECM) composition of water (70 to 80%), collagen (50 to 75%), and glycosaminoglycans (GAGs) (15 to 30%) (*3*). This composition provides cartilage with compressive, tensile, and frictional properties that enable survival and function within the biomechanically arduous joint environment.

Successful methods to regenerate bone, but not cartilage, stem from a discrepancy between the innate repair responses of these two types of tissue (Fig. 1) (*4*). A large number of cells (osteoclasts and osteoblasts) are involved in perpetual bone breakdown and remodeling. Also, the periosteum and bone marrow contain stem cells that can differentiate into bone-producing cells. Bone's extensive vascularity provides abundant nutrients and blood-borne proteins that stimulate tissue repair. Defects in bone can thus be self-repaired up to a critical size, although regeneration in large bony defects requiring vascularization continues to be a problem. In contrast to bone's cellularity, cartilage's few cells exhibit low metabolic activity. Its scarce resident stem cells, which have recently been identified, appear to require considerable in vitro manipulation to produce cartilage (*3*, *5*). Few, if any, cells are specialized in cartilage remodeling; chondroclasts have only been described for calcified or hypertrophic matrices. Cartilage is dependent on synovial fluid perfusion to meet its nutritional needs. Without cells and factors conducive to healing, even small, superficial cartilage defects fail to heal (*3*).

Current bone-regeneration products are used in cases where external support is provided by plates or cages or where the implant is not intrinsic to the stability of the bony structure. These indications allow sufficient mechanotransduction for stimulation of bone growth and, thus, successful bone regeneration, without necessarily recapitulating native biomechanical properties. For cartilage, comparable indications do not exist, and the generated tissue must be strong, yet highly deformable, and lubricious while exhibiting time-dependency in its stress-strain response. Cartilage's biomechanical environment, consisting of forces over a large range of motion, can take

Department of Biomedical Engineering, University of California, Davis, 1 Shields Avenue, Davis, CA 95616, USA.

*To whom correspondence should be addressed. E-mail: athanasiou@ucdavis.edu

Downloaded from www.sciencemag.org on December 20, 2012